Composites Part B 103 (2016) 90–97

Contents lists available at ScienceDirect

Composites Part B

journal homepage: www.elsevier.com/locate/compositesb

Experimental investigations for mechanical and metallurgical properties of friction stir welded recycled dissimilar polymer materials with metal powder reinforcement

Rupinder Singh [a], Vinay Kumar [a], Luciano Feo [b], Fernando Fraternali [b, *]

[a] Department of Production Engineering, Guru Nanak Dev Engineering College, Ludhiana, India
[b] Department of Civil Engineering, University of Salerno, Italy

A R T I C L E I N F O

Article history:
Received 26 July 2016
Accepted 8 August 2016
Available online 11 August 2016

A B S T R A C T

Friction stir welding (FSW) is one of the established processes for joining of polymers, metals and alloys. In the recent past many applications of this process have been explored. But hitherto very less has been reported on the friction stir welded joints with dissimilar polymer/plastic (DP) materials (with metal powder reinforcement). In the present work investigations have been made to perform FSW of two DP materials namely: low density polyethylene (LDPE) and high density polyethylene (HDPE). The present study of FSW for DP (LDPE and HDPE) has been performed on vertical milling machine. The effect of FSW process parameters on mechanical and metallurgical properties (such as: Shore D hardness, tensile strength and porosity of weld joint) has been investigated for structural engineering applications. The results are supported by photomicrographs.

1. Introduction

Joining of dissimilar material is needed in many engineering applications and conventional fusion welding of dissimilar material often results in defective welds. FSW has paved way for joining dissimilar materials. Defect free joints have been obtained for a number of dissimilar material combinations in case of metals and alloys [1]. In case if finished assembly is too complex or large, it is necessary to join same or different parts. FSW was invented as a novel joining technique in 1991 at The Welding Institute, Cambridge, United Kingdom [2]. This process was used to join Al alloys. In automobile and manufacturing industries, FSW is preferred to join dissimilar metals combinations. FSW enhance the mechanical properties of welded joints [3]. In many commercial applications, where industries needed panels for decks, sides etc. FSW is applicable in such industries to weld the sheets in one long run. The problem of welding similar as well as dissimilar metals, non-metals and alloys can be easily resolved by FSW on vertical milling machine setup. To produce quality products of plastic at large volumes, many techniques have been developed to join plastic based material. Due to less surface energy, presence of release agents from last processing steps and poor weldability, it is difficult to join polymers or plastic based materials. By using some reinforcement techniques in parent material welding of plastic based materials can be done successfully [4]. Miscibility of plastic based materials is studied carefully before joining DP materials. Thermodynamically, most of the DP is immiscible in nature [5]. In past FSW of polyethylene was performed on milling setup to investigate the effects on morphological properties on welds [6].

The literature review reveals that FSW of LDPE and HDPE (which is available in large quantity as waste and posing threat for environment) after reinforcement of Fe metal powder has not been investigated so far. In order to check whether these two DP can be welded to give good mechanical and metallurgical properties, the present study has been conducted. It should be noted that the glass transition temperature and melt flow index (MFI) type rheological properties of polymeric materials can be improved by reinforcement of different metal powders, which will increase the application domain of these polymeric materials [7–11].

Till now many applications of FSW process in industries have been investigated [12–17]. Sheets of virgin polyethylene such as HDPE, ABS were welded; their mechanical properties were examined and a novel approach for production of nano-composite polymer had been proposed [18–22]. The strength and weakness of FSW based polymer materials (polypropylene) and Al was checked. Metallurgical properties of joints made by FSW have been

* Corresponding author.
E-mail address: f.fraternali@unisa.it (F. Fraternali).

http://dx.doi.org/10.1016/j.compositesb.2016.08.005
1359-8368/

analyzed [23–30]. Along with morphology, tool profile and shoulder design properties were also checked for similar as well as dissimilar materials in order to optimize FSW process parameters [31–36]. Many properties like grain growth, heat transfer, tool forces and effect of threaded pin has been studied for FSW of thermoplastics [37–42].

In the present study, investigations have been made for FSW of recycled LDPE and HDPE with reinforcement of Fe powder for different structural applications.

2. Experimentation

During pilot experimentation, cylindrical shaped specimens were prepared on specimen hot mounting press by applying concept of pressure moulding. Cylindrical specimens were cut mechanically into semi-circular pieces. FSW process was carried on vertical milling machine at 1750, 1800 and 1850 RPM. Welding was unsuccessful because LDPE and HDPE do not have similar properties like molecular structure, carbon chain, glass transition temperature, intermolecular bonding and melt flow index etc. After this 10% (by weight) Fe powder reinforcement was made in HDPE and reinforcement of 10% Fe powder in LDPE pieces and FSW was performed on such samples. The reinforcement based FSW process was successful due to better metallic bonding obtained by reinforcement of Fe metal powder and appropriate melting of LDPE and HDPE at high temperature produced by stirring. So by applying concept of reinforcement for better bonding characteristics at weld joint interfaces, FSW was performed. Finally good quality of welding joint was obtained. This process of welding was successful may be the reason behind it was the bonding of Fe particles present in two specimens. Fig. 1 shows the joint prepared with 10% Fe powder reinforcement in LDPE and HDPE.

The joining of LDPE and HDPE proves that the FSW of DP material is possible if Fe powder is reinforced. It should be noted that the reinforcement increases the melt flow index (MFI) of the polymers. The aim of this pilot study was to check whether the welding of LDPE and HDPE is useful for engineering applications. To make the welding of DP possible, MFI needs to be investigated. Therefore an experiment was conducted to test MFI of LDPE and HDPE when Fe powder was reinforced.

The MFI of plastic based materials was calculated and a tabular data was generated. The Fe metal powder (available as a scrap from machining industry) of 53–60 μm was mixed at varying proportions with LDPE. MFI was measured at 230 °C temperature by applying 3.8 kg standard weight on piston rod. The same operations were carried to calculate the MFI of HDPE with reinforcement of Fe metal powder. The pilot experiment data stated in Table 1 shows that these materials don't have similar range of MFI.

Meltflow tester was used as per ASTM D 1238 standard to find MFI of LDPE and HDPE after Fe powder reinforcement. It is clear from MFI pilot study that Fe powder increases the MFI of LDPE and HDPE. So, there was a need to fix the proportion of reinforcement powder to perform FSW. At first stage FSW of reinforced LDPE with 10% Fe and HDPE with 10%Fe specimens was performed. This trial was successful as strong and hard weld joint surface was obtained. This successful welding showed that Fe metal powders may have formed metallic bonding to weld LDPE and HDPE.

After successful pilot experiment, this combination of composition/proportion of metal powder with polymer matrix have been selected for further investigations, with design of experimentation based on Taguchi L9 orthogonal array as listed in Table 2.

Based upon Table 2 and 3 shows control log of experimentation.

The output parameters for the present study are tensile strength, Shore D hardness and porosity at joint. These parameters have been selected to ascertain the functional ability of the welded joints.

3. Result and discussion

After 03 successful batch runs for each combination of metal powder reinforcement according to Taguchi L9 orthogonal array,

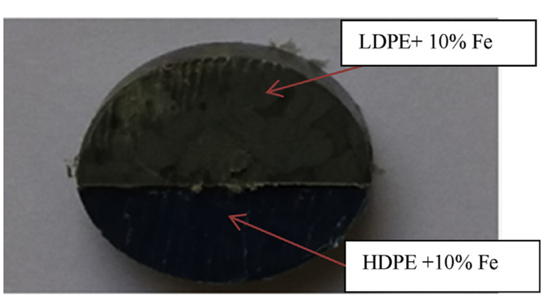

Fig. 1. Pilot experimentation of LDPE and HDPE friction stir welding.

Table 2
Parameters selected for experimentation Based on Taguchi L9 orthogonal array.

Levels	(A) Specimen thickness (mm)	(B) Feed rate (mm/rev)	(C) Rotational speed (rpm)
1	6	300	1750
2	8	325	1800
3	10	350	1850

Table 3
Control log of experimentation.

Parametric conditions	A (mm)	B (mm/rev)	C (rpm)
1	6	300	1750
2	6	325	1800
3	6	350	1850
4	8	300	1800
5	8	325	1850
6	8	350	1750
7	10	300	1850
8	10	325	1750
9	10	350	1800

Table 1
MFI with Fe powder reinforcement.

Wt. % of Al	MFI of LDPE (230 °C,3.8 kg load)	MFI of HDPE(230 °C,3.8 kg load)
0	2.37	17
10	2.69	23.64
20	3.07	22.86
30	3.01	24.64
40	2.85	26.98

the results for different output parameters like Shore D hardness, tensile strength and porosity at weld joint have been calculated.

3.1. Shore D hardness at interface

The observation of Shore D (Durometer) hardness of the welded joint is recorded in Table 4 as shown below.

The output obtained for Shore D hardness of welded specimens were analyzed on Minitab software under the condition that larger is better (see Fig. 2). It shows that specimen thickness 8 mm, supply rate 300 mm/min and rotational speed of 1800 rpm are best parameters for maximum hardness. It is because friction at high rpm generates more heat. Smaller the feed, better the intermolecular diffusion obtained at joint. Fe powder diffused very well for less supply rate. Increase in feed rate leads to reduction in hardness because Fe powder spill out at high feed. It means medium specimen thickness, lesser feed rate and high rotational speed gave best property of hardness, but least specimen thickness 6 mm, high feed rate 350 mm/min and high rotational speed of 1850 rpm for welding resulted in lowest hardness value.

Tables 5 and 6 shows the analysis of variance and ranking of input parameters (based on SN ratio) respectively.

The formula based upon Taguchi design has been used for optimization of process parameters that gave optimum hardness value of weld.

$$\eta_{opt} = x + (x_{A3} - x) + (x_{B1} - x) + (x_{C1} - x)$$

Where, $\eta_{opt}$is the optimum value of SN ratio obtained for the Shore D hardness of Fe metal powder reinforcement smaples, 'x' is the overall mean of S/N data, x_{A3} is the mean of S/N data for specimen thickness at level 3 and x_{B1} is the mean of S/N data for factor feed rate at level 1 and x_{C1} is the mean of S/N data for factor rpm for welding at level 1.

$$y^2_{opt} = (1/10)^{\eta opt/10} \quad \text{for properties where less is better}$$

$$y^2_{opt} = (1/10)^{\eta opt/10} \quad \text{for properties where more is better}$$

Calculation,

Overall mean of SN ratio (m) was taken from Minitab software $x = 33.4521\text{dB}$

Now from response table of signal to noise ratio, $x_{A3} = 33.840$, $x_{\mathbf{B1}} = 33.910$ and $x_{C1} = 33.790$

From here, $\eta_{opt} = 33.452 + (33.840 - 33.452) + (33.910 - 33.452) + (33.790 - 33.452)$

$\eta_{opt} = 34.636$ dB

Now, to optimize $y^2_{opt} = (10)^{\eta opt/10}$

$y^2_{opt} = (10)^{34.636/10}$

Table 4
Shore D hardness value at obtained weld interface (Fe metal powder reinforced).

Experimental conditions	Set of experiment 1	Set of experiment 2	Set of experiment 3
1	54	41.5	51
2	52	40	45.5
3	38	43.5	37.5
4	50.5	54.5	48
5	47.5	40.5	43.5
6	48	51.5	52.5
7	49	56.5	46.5
8	48	47.5	49.5
9	47.5	48.5	51.5

Table 5
Analysis of variance for SN ratios.

Source	DF	Seq SS	Adj SS	Adj MS	F	P	%Age contribution
A	2	1.6065	1.6065	0.8033	4.44	0.184	37.22
B	2	0.9533	0.9533	0.4767	2.64	0.275	22.09
C	2	1.3936	1.3936	0.6968	3.85	0.206	32.29
Residual Error	2	0.3618	0.3618	0.1809			8.38
Total	8	4.3153					

Table 6
Response table for signal to noise ratios (Larger is better).

Level	A	B	C
1	32.86	33.91	33.79
2	33.66	33.18	33.67
3	33.84	33.27	32.90
Delta	0.97	0.73	0.89
Rank	1	3	2

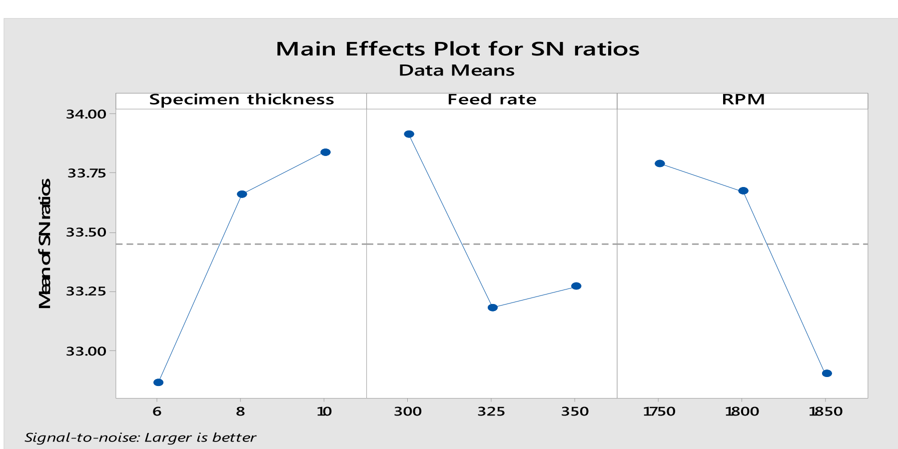

Fig. 2. Main effects plot for SN ratios of shore D hardness.

$y_{opt} = 53.92$

So, Optimum Shore D hardness = 53.92 shore D.

3.2. Tensile strength of weld pieces at joint interface

Table 7 shows the values of tensile strength obtained for Fe metal powder reinforced welded samples; tensile test was carried on universal tensile tester to generate the tabulated results of tensile strength of weld joints. To check the variations in tensile strength, the experiment was carried for 3 separate batch runs to study the role of process parameters in improving joint strength. Fig. 3 gives plot for SN ratio main effect of tensile strength. It shows that highest tensile strength for specimen thickness 10 mm, feed rate 300 mm/min and rotational speed of 1850 rpm is providing the best results. The reason is that high rpm generate more heat by friction. Due to lesser feed rate, effective intermolecular dispersion occurs at joint interface. There is appreciable diffusion of Fe powder in polymer matrix but decrease in rpm created problem of improper matrix formation of metal powder with polymer. Therefore, the tensile strength decreases. For more specimen thickness, low feed rate and high rotational speed tensile properties are quite high. On the other hand low specimen thickness of 6 mm, low feed rate 300 mm/min and rotational speed of 1750 rpm for welding resulted in lowest tensile strength.

Table 8 shows the ANOVA for SN ratios of tensile strength. 6.18% residual error was obtained. It means the predicted model has good accuracy for tensile strength than the model predicted for Shore D hardness.

Table 9 gives the response table for SN ratios of tensile strength. As observed from the table, specimen thickness given most attribute to the SN ratios and rotational speed given least attributes to the SN ratios for Fe metal powder reinforced FSW specimens.

Table 7
Tensile strength (MPa) of welded joint (Fe metal powder reinforced).

Experimental conditions	Set of experiment 1	Set of experiment 2	Set of experiment 3
1	4.975	4.638	5.012
2	7.627	7.482	7.110
3	8.405	8.609	8.287
4	8.499	8.286	8.641
5	8.951	8.921	8.624
6	10.463	11.239	9.879
7	14.875	15.194	14.258
8	14.177	14.782	14.081
9	14.653	15.025	14.201

Table 8
Analysis of variance for SN ratios.

Source	DF	Seq SS	Adj SS	Adj MS	F	P	%Age contribution
A	2	68.524	68.524	34.262	13.35	0.070	82.63
B	2	7.175	7.175	3.587	1.40	0.417	8.65
C	2	2.089	2.089	1.045	0.41	0.711	2.51
Residual Error	2	5.132	5.132	2.566			6.18
Total	8	82.920					

Table 9
Response table for signal to noise ratios (Larger is better).

Level	A	B	C
1	16.55	18.56	19.09
2	19.30	19.81	19.75
3	23.27	20.74	20.27
Delta	6.72	2.18	1.18
Rank	1	2	3

Optimization for tensile strength (Fe metal powder reinforcement)

As optimization was done for Shore D hardness value, in case of tensile strength same procedure were followed for optimization and it was calculated as 14.52 MPa for Fe metal powder reinforced FSW samples. It is calculated as per following procedure:

$$\eta_{opt} = x + (x_{A3} - x) + (x_{B3} - x) + (x_{C3} - x)$$

where, η_{opt} is the optimum value of SN ratio obtained for the Tensile strength of Fe metal powder reinforcement samples.'x' is the overall mean of S/N data, x_{A3} S/N mean data for specimen thickness at level 3 and x_{B3} is the mean of S/N data for factor feed rate at level 3 and x_{C3} is the mean of S/N data for factor rpm for welding at level 3.

$$y^2_{opt} = (1/10)^{\eta opt/10} \quad \text{property in which lower is better}$$

$$y^2_{opt} = (1/10)^{\eta opt/10} \quad \text{property in which higher is better}$$

Calculation,

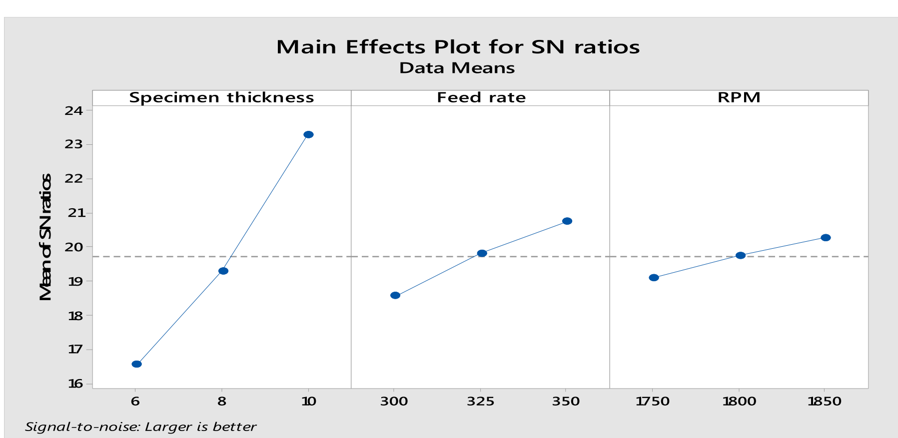

Fig. 3. Main effects plot for SN ratios of tensile strength.

On the whole mean of SN ratio (x)
was taken from Minitab software $\quad x = 19.703\text{dB}$

Now from response table of signal to noise ratio, $x_{A3} = 23.270$, $x_{B3} = 20.740$ and $x_{C3} = 20.270$

From here, $\eta_{opt} =$
$19.703 + (23.270 - 19.703) + (20.740 - 19.703) + (20.270 - 19.703)$

$\eta_{opt} = 24.874$ dB
Now, to optimize $y^2_{opt} = (10)^{\eta opt/10}$
$y^2_{opt} = (10)^{24.874/10}$
$y_{opt} = 14.52$

So, Optimum Tensile strength for Fe powder reinforced specimens = 14.52 MPa.

3.3. Porosity percentage at joint interface

Table 10 shown the values obtained for the samples whose %age porosity is listed after Fe metal powder reinforced specimen was joined. The data in the table is output of optical micrographs test conducted by using MIAS software for the process parameters selected as per Table 3. Fig. 4 is shows SN ratio main effect for %age porosity at joint. As observed from Fig. 4 for good porosity specimen thickness 6 mm, feed rate 350 mm/min and rotational speed of 1850 rpm are providing the best results. Good result obtained due to formation of better metal polymer matrix and lesser heat formation, the 350 mm/min of feed rate given less porous joint because metal polymer matrix formation occur at such stages. The low specimen thickness of 6 mm at high feed produced effective diffusion of Fe powder in polymer matrix. As low specimen thickness, high feed rate and high rotational speed are responsible for the better porosity of welds. In the same way combination of specimen thickness 8 mm, feed rate 350 mm/min and rotational speed of 1750 rpm for welding results in poorest porosity at joint interface.

Table 11 shows tabular data obtained for porosity percentage at joint interface of weld. It gives the value of analysis of variance for SN ratios obtained for porosity at joint. Output of 5.37% residual error reveals that high accuracy has been achieved for porosity in the proposed model when FSW is performed with reinforced Fe metal powder in dissimilar plastic based material.

Table 12 represents obtained values of the porosity %age at joint interface for the response table of SN ratios. According to the delta and rank values of table, topmost attribute is given to the SN ratios of tool rpm and least rank is allotted to feed rate SN ratio.

Optimization for porosity percentage (Fe metal powder reinforcement)

As optimization was carried out for Shore D hardness value, in case of %age porosity at joint interface, same procedure were followed for optimization of Fe metal powder reinforcement samples. It is calculated as per following procedure:

Table 10
%Age Porosity obtained at weld joint (Fe metal powder reinforced).

Experimental conditions	Set of experiment 1	Set of experiment 2	Set of experiment 3
1	26.13	26.57	25.81
2	16.06	16.79	15.68
3	11.41	12.01	12.84
4	18.82	19.85	20.25
5	14.84	16.98	15.56
6	27.26	27.67	26.31
7	18.13	19.86	21.77
8	23.75	25.58	24.37
9	17.09	19.87	20.64

Table 11
Analysis of variance for SN ratios.

Source	DF	Seq SS	Adj SS	Adj MS	F	P	%Age contribution
A	2	5.323	5.323	2.661	2.36	0.297	12.70
B	2	4.002	4.002	2.001	1.78	0.360	9.55
C	2	30.305	30.305	15.153	13.45	0.069	72.35
Residual Error	2	2.253	2.253	1.127			5.37
Total	8	41.882					

Table 12
Response table for signal to noise ratios (Smaller is better).

Level	A	B	C
1	−24.73	−26.74	−28.27
2	−26.17	−25.33	−25.25
3	−26.50	−25.33	−23.88
Delta	1.77	1.42	4.39
Rank	2	3	1

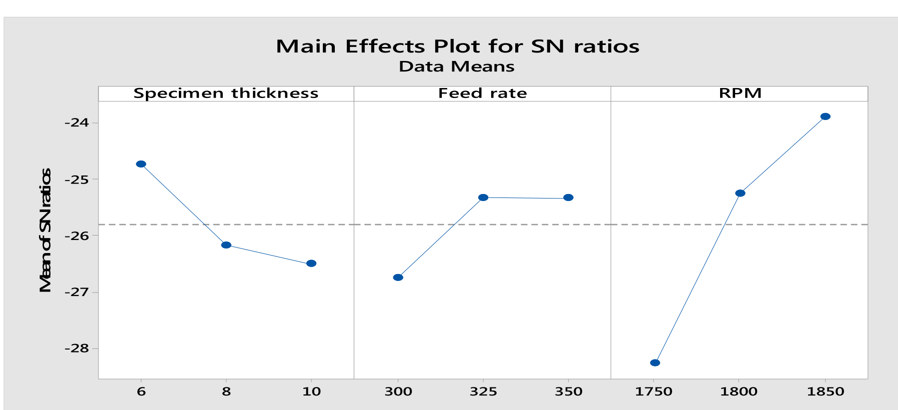

Fig. 4. Main effects plot for SN ratio.

$\eta_{opt} = x + (x_{A3} - x) + (x_{B1} - x) + (x_{C1} - x)$

Where, $\eta_{opt}$is the optimum value of SN ratio obtained for the Porosity of Fe metal powder reinforcement smaples.'x' is the overall mean of S/N data, x_{A3} is the mean of S/N data for specimen thickness at level 3 and x_{B1} is the mean of S/N data for factor feed rate at level 1 and x_{C1} is the mean of S/N data for factor rpm for welding at level 1.

$$y^2_{opt} = (1/10)^{\eta opt/10} \quad \text{properties in which lower is better}$$

$$y^2_{opt} = (1/10)^{\eta opt/10} \quad \text{properties in which higher is better}$$

Calculation,

Overall mean of SN ratio (x) was taken from Minitab software $x = -25.801\text{dB}$

Now from response table of signal to noise ratio, $x_{A3} = -26.50$, $x_{B1} = -26.74$ and $x_{C1} = -28.27$

From here, $\eta_{opt} = -25.801 + (-26.50 - (-25.801)) + (-26.74 - (-25.801)) + (-28.27 - (-25.801))$

$\eta_{opt} = -29.08$ dB
Now, to optimize $y^2_{opt} = (1/10)^{\eta\ opt/10}$
$y^2_{opt} = (0.1)^{-29.08/10}$
$y_{opt} = 18.26$

The optimum porosity for Fe powder reinforced sample = 18.26%.

Fig. 5 shows photo micrographs observed for welded samples according to the different set of parameters selected as per the control log of experimentation given in Table 3.

As observed from Fig. 5, friction stir welded LDPE and HDPE joint produced (after reinforcement of Fe powder) has more uniform dispersion of Fe particles which resulted into better mechanical properties thus making it useful for many structural applications. The micrograph was examined at 100× magnification. The results of porosity obtained in Table 10 are supported by the images shown in Fig. 5. For experimental setup 3, minimum porosity is observed when specimen thickness was 6 mm, 350 mm/

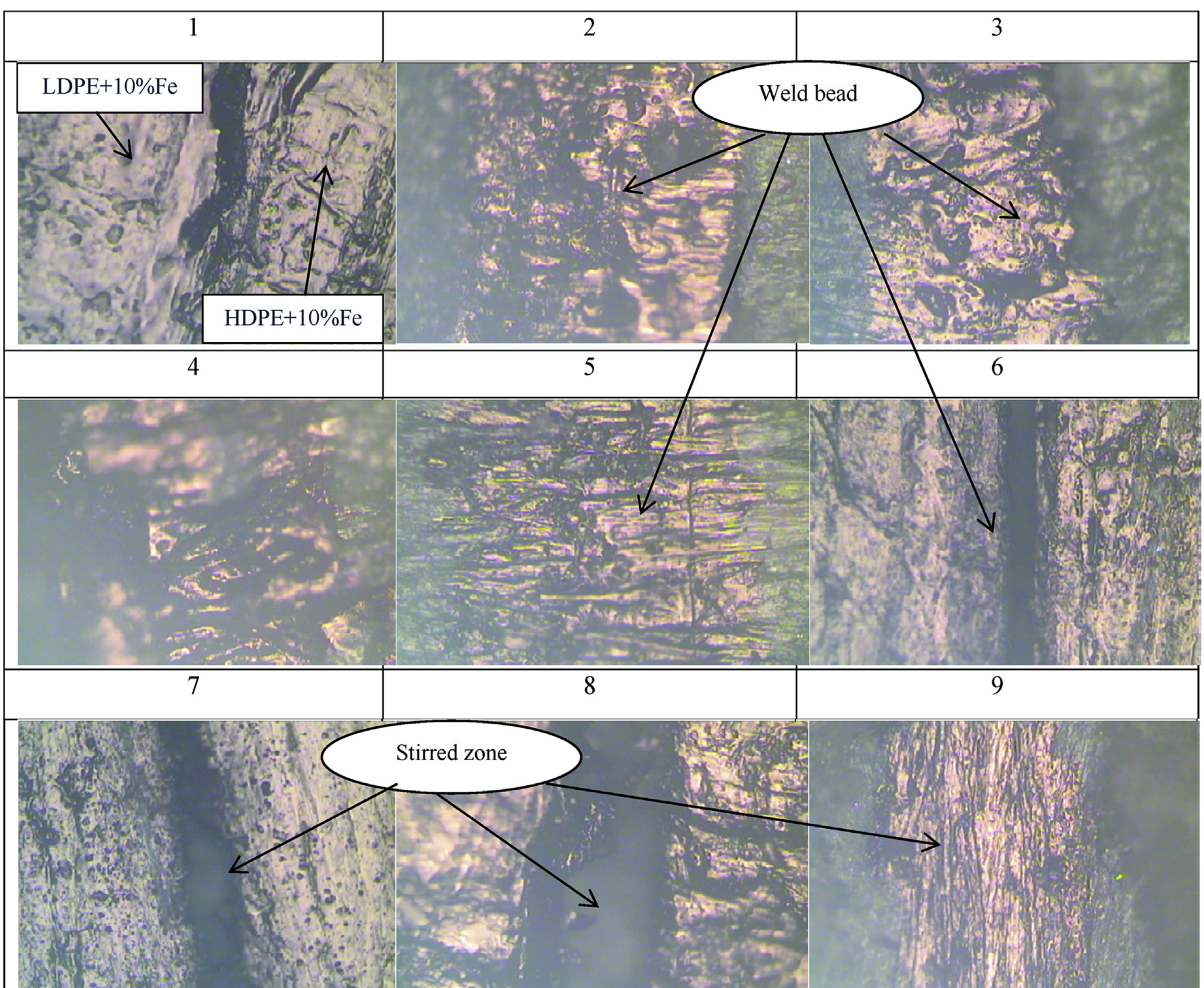

Fig. 5. Optical micrographs for reinforced Fe powder joints (at magnification of 100×).

rev was the feed rate and rotational speed was 1850RPM which shows better dispersion of Fe particles.

4. Conclusions

- It is observed that recycled LDPE and HDPE polymers can be welded by FSW Process.
- The reinforcement of Fe metal powder produced a metallic bonding at joint interface of LDPE and HDPE that provided a good joint strength.
- It is necessary to establish a range of melt flow index (MFI) for friction welding of plastic materials. But, in friction stir welding process, plastic materials can be welded by coalescence caused due to stirring of material since rotary and traverse motion of tool increases the temperature and melts the work pieces.
- The mechanical properties obtained of the weld after reinforcing Fe powder are more than the mechanical properties of the parent material.
- The maximum53.92 Shore D hardness is obtained in experiment no. 4 where 8 mm specimen thickness, 300 mm/min feed rate and 1800 rpm of tool were the parametric combination. This hardness obtained because of better intermolecular diffusion of metal and plastic material where feed rate conditions were low.
- The highest14.52 MPa tensile strength in experiment no. 9 has been obtained in which 10 mm specimen thickness, 350 mm/min feed rate and 1800 rpm of tool were selected parameters. The formation of better metal polymer matrix resulted in better tensile strength at peak under the low feed rate conditions.
- The minimum porosity of 11.41% is obtained in experiment no. 3 in which 6 mm specimen thickness, 350 mm/min feed rate and 1850 rpm of tool were the parametric combinations. The observation was due to the fact that few spaces formed at interface of the joint after attaining high feed rate and high tool rpm situation.

Future directions of the present research might regard the use of FSW for the manufacturing of high-performance reinforcements of composite materials [43–51], and novel mechanical metamaterials [52–55].

Acknowledgement

The authors would like to thank Manufacturing Research Lab (Production Engineering, GNDEC Ludhiana) and Institution of Engineers (India), Grant Number: PG2016011 for providing financial support to this project.

References

[1] Padmanban V, Kishore VR, Balusamy V. Numerical Simulation of Temperature Distribution and Material Flow During Friction Stir Welding of Dissimilar Aluminium Alloys. 12th Global Congress on Manufacturing and Management (2016), GCMM, Procedia Eng, 97, pp. 854–863.
[2] Gao J, Chao Li, Shilpakar U, Shen Y. Improvements of mechanical properties in dissimilar joints of HDPE and ABS via carbon nanotubes during friction stir welding process. Mater Des 2015;86:289–96.
[3] Shen Z, Chen Y, Haghshenas M, Gerlich AP. Role of welding parameters on interfacial bonding in dissimilar steel/aluminium friction stir welds. Int J Eng Sci Technol 2015;18:270–7.
[4] Kumar R. Investigating the effect of process parameters on mechanical and metallurgical properties of friction welded reinforced dissimilar plastic materials. Thesis titled. 2016.
[5] Abibe AB, Sonego M, Santos JF, Canto LB, Amancio-filho ST. On the feasibility of a friction based staking joining method for polymer-metal hybrid structures. Mater Des 2015. http://dx.doi.org/10.2016/j.matdes.2015.12.087.
[6] Arici A, Selale S. Effect of tool tilt angle on tensile strength and fracture location of friction stir welding of polyethylene. Sci Technol Weld Join 2007;12:536–9.
[7] Kolbasuk GM. Hot wedge fusion welding of HDPE geomembranes. GeotextGeomembranes 1990;9(4–6):305–17.
[8] Kumar N, Yuan W, Mishra RS. Friction stir welding of dissimilar alloys and materials. Oxford, UK: Butterworth-Heinemann; 2015. Chap. 2.
[9] Mercana S, Aydin S, Ozdemir N. Effect of welding parameters on the fatigue properties of dissimilar AISI 2205–AISI 1020 joined by friction welding. Int J Fatigue 2015;81:78–90.
[10] Su JQ, Nelson TW, Sterling CJ. Friction stir processing of large area bulk UFG aluminum alloys. Scr Mater 2005;52(2):135–40.
[11] Singh R, Singh S, Fraternali F. Development of in-house composite wire based feed stock filaments of fused deposition modelling for wear-resistant materials and structures. Compos Part B Eng 2016;98:244–9.
[12] Ahmadkhaniha D, Asadi P. Mechanical alloying by friction stir processing. 2014. http://dx.doi.org/10.1533/9780857094551.387.
[13] Amini A, Asadi P, Zolghadr P. Friction stir welding applications in industry. 2014. http://dx.doi.org/10.1533/9780857094551.671.
[14] Anna SE, Giuseppe B, Alessandro G, Fabrizio Q. Friction stir welding of polyethylene sheets. Mater Des 2009;13:782–9.
[15] Azarsa E, Mostafapour A. Experimental investigation on flexural behaviour of friction stir welded high density polyethylene sheets. J Manuf Process 2014;16:149–55.
[16] Bagheri A, Azdast T, Doniavi A. An experimental study on mechanical properties of friction stir welded ABS sheets. Mater Des 2012;43:402–9.
[17] Barmouz M, Seyfi J, Givi MKB, Hejazi I, Davachi SM. A novel approach for producing polymer nano-composites by in-situ dispersion of clay particles via friction stir processing. Mater Sci Eng A 2011;528:3003–6.
[18] Barmouz M, Shahi P. Friction stir welding/processing of polymeric materials. 2014. http://dx.doi.org/10.1533/9780857094551.601.
[19] Bilici MK. Effect of welding parameters on fracture mode and weld strength friction stir spot welds of polypropylene sheets. New Tech Ganati; 2010. p. 841–4. paper no. ESDA 2010-25344.
[20] Bussu G, Irving PE. The role of residual stress and heat affected zone properties on fatigue crack propagation in friction stir welded 2024-T351 aluminium joints. Int J Fatigue 2003;25:77–88.
[21] Czigany T. Microscopic analysis of the morphology of seams in friction stir welded polypropylene. Express Polym Lett 2012;6:54–62.
[22] Davoodi A, Esfahani Z, Sarvgarh M. Microstructure and corrosion characterization of the interfacial region in dissimilar friction stir welded AA5083 to AA 7023. Corros Sci 2016. http://dx.doi.org/10.1016/j.corsci.2016.02.027.
[23] Eslami S, Ramos T, Tavares Paulo J, Moreira PMGP. Shoulder design developments for friction stir welding lap joints of dissimilar polymers. J Manuf Process 2015;20:15–23.
[24] Essa GMF, Zakria HM, Mahmoud TS, Khalifa TA. Microstructure examination and micro hardness of friction stir welded joint of AA7020-O after PWHT. Housing and Building National Research Centre. HBRC J 2015;20:376–83.
[25] Gharacheh MA, Kakobi AH, Daneshi GH, Shalchi B, Sarrafi R. The influence of the ratio of "rotational speed/traverse speed"($\omega/\bar{\upsilon}$) on mechanical properties of AZ31 friction stir welds. Int J Mach Tools Manuf 2006;46:1983–7.
[26] Gibson BT, Lammlein DH, Prater TJ, Longhurs WR. Introduction to the basic principles of friction stir welding as well as survey of the latest research and application in the field. J Manuf Process 2008;14:256–76.
[27] Giraud L, Robe H, Claudina C, Desrayaud C, Bocherd P, Feulvarch E. Investigation into the dissimilar friction stir welding of AA7020-t651 and AA6060-t6. J Mater Process Technol 2016;235:220–30.
[28] Jaiganesh V, Maruthu B, Gopinath E. Optimization of process parameters on friction stir welding of high density polypropylene plates. 12th Global Congress on Manufacturing and Management(2014), GCMM, Procedia Eng, 97, pp.1957–1965.
[29] Kumar AP, Raj R, Kailas SV. A novel in –situ polymer derived nano ceramic MMC by friction stir processing. Mater Des 2015;85:626–34.
[30] Malik V, Sanjeev NK, Suresh Hebbar H, Satish VK. Investigations of the effect of various tool pin profiles in friction stir welding using finite element simulations. Procedia Eng 2014;97:1060–8.
[31] Mendez Patricio F, TelloKarem E, Liener Thomas J. Scaling of coupled heat transfer and plastic deformation around the pin in friction stir welding. Act a Mater 2010;58:6012–26.
[32] Moataz M Attallah, Salem Hanadi G. Friction stir welding parameters: a tool for controlling abnormal grain growth during subsequent heat treatment. Mater Sci Eng A 2005;391(1–2):51–9.
[33] Panneerselvam K, Lenin K. Effects and defects of the polypropylene plate for different parameters in friction stir welding process. IJRET 2013;2:143–52.
[34] Pannneerselvam K, Lenin K. Effect of tool forces and joint defects during friction stir welding of polypropylene plates. Int Conf Model Optim Comput Eng 2012;38:3927–40.
[35] Pannneerselvam K, Lenin K. Joining of nylon 6 plates by friction stir welding process using threaded pin profile. Mater Des 2014;53:302–7.
[36] Paoletti A, Lambiase F, Ilio AD. Optimization of friction stir welding of thermoplastics. In: 9th CIRP conference on intelligent computation in manufacturing engineering; 2014. CIRP CIME'14.
[37] Payganeh GH, Mostafa Arab NB, Asif YD. Effects of friction stir welding process parameters on appearance and strength of polypropylene composite welds. Int J Phys Sci 2011;6(19):4595–601.
[38] Romeis S, Schmidt J, Peukert W. Mechanochemical aspects in wet stirred media milling. Int J Milling Process 2016.
[39] Saeedy S, Besharati MK. Effects of critical process parameters of friction stir welding of polyethylene. Part B J Manuf Eng 2011;225:1305–10. Proceedings of the Institution of Mechanical Engineers.

[40] Simoes F, Rodrigues DM. Material flow and thermo mechanical conditions during friction stir welding of polymers: literature review, experimental results and empirical analysis. Mater Des 2013;13:261–8.
[41] Vijendra B, Sharma A. Induction heated tool assisted friction stir welding (i-FSW): a novel hybrid process for joining of thermoplastics. J Manuf Process 2015;20:234–44.
[42] Williamson KM. A moving boundary formulation for recursive plastic heat release during friction stir welding. J Mater Process Technol 2006;180:49–52.
[43] Singh R, Singh S, Fraternali F. Development of in-house composite wire based feed stock filaments of fused deposition modelling for wear-resistant materials and structures. Compos Part B, Eng 2016;98:244–9.
[44] Singh R, Kumar R, Feo L, Fraternali F. Friction welding of dissimilar plastic/polymer materials with metal powder reinforcement. Compos Part B, Eng 2016;101:77–86.
[45] Fraternali F, Farina I, Polzone C, Pagliuca E, Feo L. On the use of R-PET strips for the reinforcement of cement mortars. Compos Part B, Eng 2013;46:207–10.
[46] Farina I, Fabbrocino F, Carpentieri G, Modano M, Amendola A, Goodall R, et al. On the reinforcement of cement mortars through 3D printed polymeric and metallic fibers. Compos Part B, Eng 2016;90:76–85.
[47] Farina I, Fabbrocino F, Colangelo F, Feo L, Fraternali F. Surface roughness effects on the reinforcement of cement mortars through 3D printed metallic fibers. Compos Part B, Eng 2016;99:305–11.
[48] Fabbrocino F, Farina I, Amendola A, Feo L, Fraternali F. Optimal design and additive manufacturing of novel reinforcing elements for composite materials. In: ECCOMAS congress 2016 – European congress on computational methods in applied sciences and engineering, 5–10 june 2016; 2016. Crete Island, Greece, No. 4544 (16 pages).
[49] Kim B, Doh JH, Yi CK, Lee JY. Effects of structural fibers on bonding mechanism changes in interface between GFRP bar and concrete. Compos Part *B, Eng* 2013;45(1):768–79.
[50] Donnini J, Corinaldesi V, Nanni A. Mechanical properties of FRCM using carbon fabrics with different coating treatments. Compos Part B, Eng 2016;88:220–8.
[51] Jia Y, Chen Z, Yan W. A numerical study on carbon nanotube pullout to understand its bridging effect in carbon nanotube reinforced composites. Compos Part B, Eng 2015;81:64–71.
[52] Amendola A, Nava EH, Goodall R, Todd I, Skelton RE, Fraternali F. On the additive manufacturing and testing of tensegrity structures. Compos Struct 2015;131:66–71.
[53] Amendola A, Smith CJ, Goodall R, Auricchio F, Feo L, Benzoni G, et al. Experimental response of additively manufactured metallic pentamode materials confined between stiffening plates. Compos Struct 2016;142:254–62.
[54] Amendola A, Fabbrocino F, Feo L, Fraternali F. Dependence of the mechanical properties of pentamode materials on the lattice microstructure. In: ECCOMAS congress 2016 – European congress on computational methods in applied sciences and engineering, 5–10 june 2016; 2016. Crete Island, Greece, No. 6004 (17 pages).
[55] Amendola A, Carpentieri G, Feo L, Fraternali F. Bending dominated response of layered mechanical metamaterials alternating pentamode lattices and confinement plates. Compos Struct 2016. http://dx.doi.org/10.1016/j.compstruct.2016.07.031. Online first:.